The flow into an expanding spherical vortex

By J. S. TURNER

Division of Radiophysics, CSIRO, Sydney, Australia†

(Received 1 May 1963)

A kinematic model of the flow around and into a buoyant 'thermal' is discussed in some detail, and compared with existing laboratory observations. The basic assumption is that the flow is instantaneously the same as it is for Hill's spherical vortex of fixed size moving through a frictionless fluid. The equations describing the motion of a particle have been modified to allow for an expansion in radius proportional to the distance travelled, and a numerical integration of these time-dependent equations has been performed in order to find particle trajectories, with respect to both the instantaneous boundary of the spherical vortex and axes at rest. It is shown that for the expanding vortex there is no quantity corresponding to the 'drift distance' or the total forward displacement of particles in the flow round a sphere of constant size; particles in the wake of an expanding vortex have a finite forward velocity at large times.

The model gives very close agreement with the observed behaviour of particles entering a turbulent buoyant thermal, except that in the laboratory measurements the region containing the turbulent fluid resembles an oblate spheroid rather than a sphere. The thin mixing layer over the front and the addition of fluid over a broad region at the rear of a thermal, as well as the detailed particle trajectories, can all be explained as consequences of this mean velocity distribution.

1. Introduction

When an isolated element of buoyant fluid is released into a uniform environment which is at rest, it is observed that the buoyant region becomes turbulent, and spreads out as it advances under the action of gravity, due to the incorporation of fluid from the environment. The increase in radius is linear with distance, with a half-angle of spread of about 15°. A linear spread can be predicted using dimensional arguments (Scorer 1957) or it can alternatively be regarded as a necessary consequence of the increase of momentum of the moving region which is produced by the action of buoyancy (Turner 1957).

The detailed nature of the mean motion in and around such an element has been studied experimentally by Woodward (1959) and more recently by Saunders (1962). A vortex-like circulation is seen to be superimposed on the upward motion, with the shape and mean velocity distributions remaining similar with height. Miss Woodward has plotted vertical and horizontal

† At present on leave at the Woods Hole Oceanographic Institution, Woods Hole, Massachusetts.

velocity distributions and also the paths of particles relative to the 'thermals' (as the buoyant elements have been called). These show that some external fluid is incorporated by mixing into the front of the thermal, while the remainder enters from the rear. Saunders (1962) has taken streak photographs which allow one to trace streamlines relative to axes at rest; one of his photographs is reproduced in figure 1, plate 1.

Since the first publication of this description of the thermal, it has often been remarked that the observed instantaneous distribution of velocity in and around the element is very close to that in the spherical vortex described by Hill (see Lamb 1932). Hill showed that by choosing a certain form for the distribution of vorticity inside a spherical region of fluid, a solution of the equations of motion can be obtained which represents a vortex moving with constant velocity and size through inviscid surroundings. The flow outside the sphere is the same as the potential flow round a solid sphere, and the velocity components are continuous at the boundary. Levine (1959) has in fact based his theoretical model of a thermal on this idea, but he restricted his discussion to the case of a vortex of constant size, which is interchanging fluid with the environment in some unspecified way.

So far, then, the spherical vortex model has not been combined explicitly with the increase in size which is observed experimentally in still surroundings. In this paper we shall investigate to what extent the detailed experimental results can be explained in terms of an *expanding* spherical vortex. We shall first compare (in more detail than has been done previously) the observed instantaneous motion with that implied by Hill's vortex, and then study the kinematics of the mean flow around and into a vortex whose size is increasing linearly with distance.

A little more should perhaps be said first about some of the properties of the flow in a real fluid, to show that these can be adequately represented by the theoretical model. It is not immediately obvious how a description in terms of an inviscid fluid of constant density can be related to a motion which is in fact produced by buoyancy acting on a region of turbulent fluid.

The condition for axisymmetric inviscid motion is that the quantity ω/y (where ω is the azimuthal vorticity component and y is the distance from the axis) is conserved following a particle. Hill showed that this is zero outside the sphere and equal to $15U/2a^2$ inside, and so long as the radius a is constant, a steady solution with velocity U is possible in which the sum of the strengths of all the vortex filaments comprising the vortex (i.e. the circulation around it) is $5Ua$. When fluid is crossing the boundary and both the size and the velocity are changing, the continued use of the model implies that some mechanism not considered in the inviscid solution must be producing a discontinuous increase of vorticity at the edge, and a changing value inside the spherical region.

Both these effects can be explained in terms of the turbulent nature of the interior flow. The sudden change of vorticity at the boundary may be likened to that at the edge of a turbulent jet, where there is a sharp boundary between rotational and irrotational fluid, and entrained fluid quickly comes to share the vorticity of the interior. The possibility of similar mean flow distributions at

all times is also easier to understand when we use the ideas of similarity and self-preservation developed for turbulent flows. These imply that the motion can be described in terms of the variation of the mean flow properties, U and a, with time, and certain non-dimensional distribution functions which depend only on the position relative to the expanding boundary.

Now the dependence of quantities such as the circulation on the parameters U and a must on dimensional grounds be of the same form as it is in the steady inviscid model, so from this point of view the descriptions are equivalent. The existence of buoyant fluid, however, gives a mechanism which allows the changes in U and a to be predicted. For the thermal with constant total buoyancy, for example, it can be shown that the spread is linear with distance and that $U \propto a^{-1}$, so that in this case in fact the circulation (and the Reynolds number) remain constant.

The dynamical reason for the existence of a velocity distribution close to the one appropriate to steady motion is of course a different and more difficult question which will not be considered here. The use of Hill's solution amounts to the assumption that the distribution of ω is little affected by the expansion and mixing, or that at any instant the differences of ω/y from a constant value at any point in the sphere will be small.

2. The field of motion relative to axes at rest

The first comparison between the spherical vortex model and experiment may be made very simply, without the need to consider the expansion, by plotting standard results in slightly different forms from the usual ones. The basic assumption which will be made in following sections is that at any instant the motion inside a spherical region is that described by Hill, while outside it is just the potential flow around a sphere. The streamlines for this combination, with respect to axes at rest relative to the fluid at infinity, are shown in figure 2. They may be compared with the streak picture of figure 1, which gives an approximate representation of the streamlines in the laboratory thermal when the exposure time is not too long. Note that the calculated streamlines near the stagnation point tend to be more elongated than those observed, suggesting that the laboratory thermal is more flattened—as is indeed suggested by its outline. Otherwise the two pictures are very similar, and show the same symmetry of the motion at the front and rear.

A more sensitive comparison of theory and experiment may be made by plotting the vertical and horizontal components of velocity (i.e. in the direction of motion and parallel to it), again with respect to axes at rest. This has been done for Hill's spherical vortex in figure 3. While the streamlines of figure 2 are smooth and therefore the velocities are continuous, the velocity gradients are not, because of the discontinuity in the vorticity distribution present in this model. This is in strong contrast to the corresponding experimental results, as interpreted by Miss Woodward in her figure 2, where smooth velocity contours are shown. It is difficult to judge from this comparison alone whether discontinuous gradients may occur or not, since averaging over several particles

in a turbulent flow will always tend to produce a smoothing. The effect of these differences on other properties of the flow must be small, as our later calculations will show.

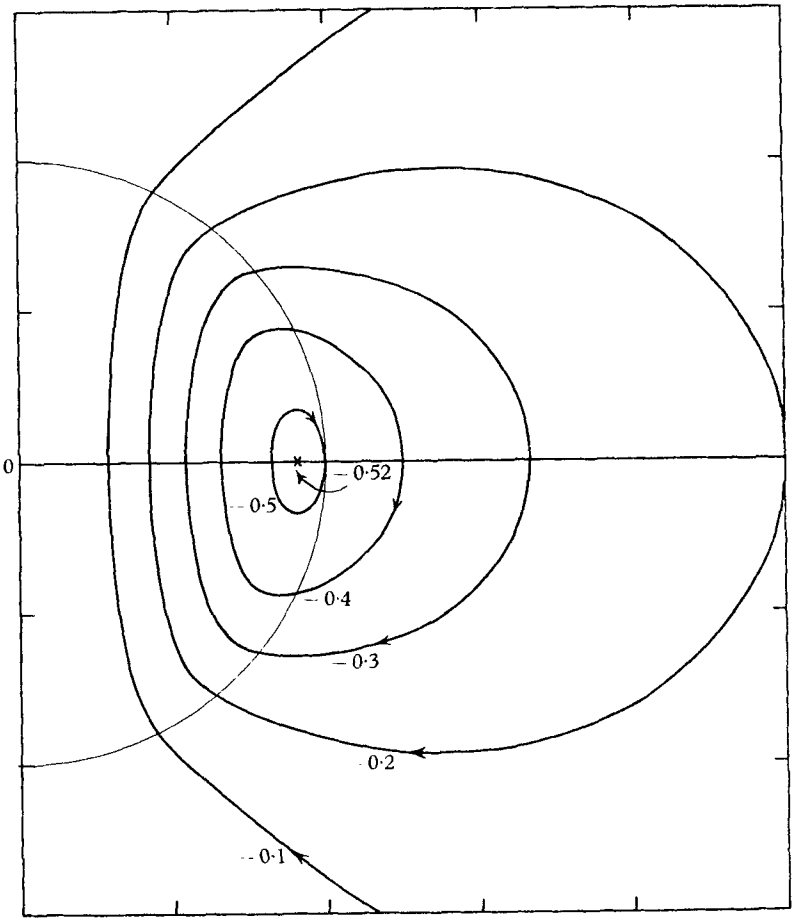

FIGURE 2. Streamlines of the flow, relative to axes at rest, of the motion in and around Hill's spherical vortex. Contours are plotted for one half of the symmetrical flow, in a plane through the axis and at equally spaced values of the Stokes stream function. Compare with figure 1, plate 1.

3. Motion relative to an expanding vortex

The time-dependent nature of the flow we wish to study introduces complications which are not often considered in classical hydrodynamics. For steady flows it has become customary to eliminate the time dependence and to calculate only the form of the streamlines. It is possible, however, to obtain extra information by leaving this time dependence in explicitly, and Morton (1913), for example, calculated detailed particle paths for several well-known flows. Darwin (1953) approached the problem more generally and showed how the 'drift' of particles, i.e. the total distance moved during the passage of a solid body, is related to the virtual mass.

Of most direct interest to us is the work of Lighthill (1956), who carried out the corresponding calculations for a sphere of fixed size. In addition to streamlines, he plotted surfaces of constant 'drift function', which are the shapes into

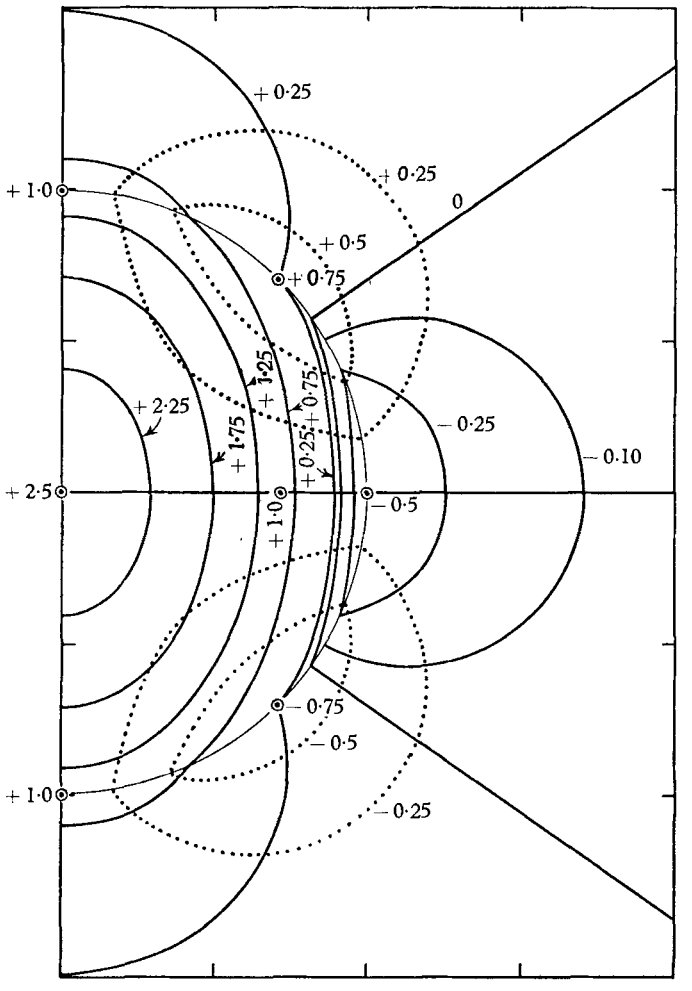

FIGURE 3. The calculated velocity distribution in and around Hill's spherical vortex. Contours of vertical velocity (solid lines) and horizontal velocity (dotted) are shown, for the right-hand side of the symmetrical flow. The values on the curves are multiples of the vertical velocity of the centre of the vortex. The numbers have been chosen so that when they are converted to multiples of the velocity of the cap (by multiplying by 0·8 for $\alpha = \frac{1}{4}$) they are the same as those used by Woodward (1959).

which planes of fluid initially at right angles to a uniform stream will be distorted as they pass over the sphere. Together, these two sets of curves show not only what happens to each particle of fluid, but *when*. In particular, they reveal that initially plane surfaces become tightly wrapped round the front of the sphere, which suggests that if the sphere were expanding, these surfaces would be incorporated into the moving volume.

The previous calculations for a sphere of constant size may be extended as follows. Consider first the motion outside the sphere. The potential-flow solution in spherical polar co-ordinates, representing a flow with unit velocity past a sphere of fixed radius a, is

$$\left.\begin{aligned} v_r &= dr/dt = -(1-a^3/r^3)\cos\theta, \\ v_\theta &= r(d\theta/dt) = (1+a^3/2r^3)\sin\theta, \end{aligned}\right\} \tag{1}$$

where r is the radius vector and θ is the angle measured from the direction of the approaching stream. We shall assume that the motion of a particle near an expanding sphere is instantaneously the same as it would be near a fixed sphere of the same size. An equivalent assumption is already implied in the usual treatments of potential flow round bodies of fixed size, when the motion at all points of the fluid is then supposed to respond instantaneously to changes of velocity of the body. In a co-ordinate system which is at rest relative to the centre of the sphere, the expansion of a moving sphere proportional to distance travelled is represented by

$$a = \alpha t U = \alpha t, \tag{2}$$

where α is a constant, the tangent of the half angle of spread, and the velocity U is again taken as unity. Combining (1) and (2) we have therefore

$$\frac{dr}{dt} = -\left(1-\frac{\alpha^3 t^3}{r^3}\right)\cos\theta, \quad \frac{d\theta}{dt} = \left(1+\frac{\alpha^3 t^3}{2r^3}\right)\frac{\sin\theta}{r}, \tag{3}$$

for the motion of a fluid particle past an expanding sphere.

It will be convenient to plot the paths of particles relative to the current radius of the sphere, or with respect to the sphere regarded as fixed in size. With the change of variable

$$\rho = r/\alpha t, \tag{4}$$

the equations (3) become

$$\left.\begin{aligned} \frac{d\rho}{dt} &= -\frac{1}{\alpha t}\left\{\alpha\rho + \left(1-\frac{1}{\rho^3}\right)\cos\theta\right\}, \\ \frac{d\theta}{dt} &= \frac{\sin\theta}{\rho\alpha t}\left(1+\frac{1}{2\rho^3}\right). \end{aligned}\right\} \tag{5}$$

Note that even in the expanding case, the time dependence could be eliminated from these equations if we were interested only in the form of the relative streamlines and not the position of particles at given times. The integration of this pair of equations may be started with any convenient set of initial conditions on ρ, θ and t, and continued until ρ becomes less than unity, which it may do if the particle enters the sphere.

A similar extension may be made to the equations for the *interior* motion in a spherical vortex. Hill's solution with $U = 1$ is

$$\left.\begin{aligned} v_r &= \tfrac{3}{2}(1-r^2/a^2)\cos\theta, \\ v_\theta &= -\tfrac{3}{2}(1-2r^2/a^2)\sin\theta. \end{aligned}\right\} \tag{6}$$

Making again the substitutions corresponding to the relative motion in an expanding co-ordinate system, $a = \alpha t$ and $\rho = r/a$, these equations become

$$\left.\begin{aligned} \frac{d\rho}{dt} &= \frac{1}{\alpha t}\{-\alpha\rho + \tfrac{3}{2}(1-\rho^2)\cos\theta\}, \\ \frac{d\theta}{dt} &= \frac{3}{2}\frac{\sin\theta}{\rho\alpha t}\{2\rho^2 - 1\}. \end{aligned}\right\} \tag{7}$$

When the integration of (5) shows that a particle has entered the spherical vortex, the motion for $\rho < 1$ may be followed using (7), with initial conditions provided by the final values obtained from the exterior calculation. This process of integration automatically insures that continuity is preserved across the boundary of the vortex.

4. Numerical solutions for the relative motion

In principle, the equations for flow near an expanding vortex are hardly more complex than those tracing particle motions round a sphere of constant size. In practice, however, it is no longer possible to obtain analytic solutions even for special ranges of the variables, and we have therefore used a high-speed computer to integrate (5) and (7). Most of the results have been obtained for $\alpha = \frac{1}{4}$, which is close to values observed in laboratory experiments, but later some of the changes introduced by using a different value of α will be considered.

The main results of this paper are presented in figure 4. As discussed in the preceding section, the paths of various particles lying initially on a plane some distance ahead of the sphere and perpendicular to its direction of travel are plotted relative to the instantaneous outline of the sphere. The points marked are separated by equal intervals of t. It is seen that a typical particle lying close to the axis enters the front of the sphere, while particles further off the axis may enter from the rear, or eventually fail to enter. Another method of presenting the same results is shown on the left of this diagram; here we have joined points having constant t, so that again these lines represent the shapes into which previously plane surfaces are distorted by the mean motion around and inside the spherical vortex. Both these plots are immediately suggestive of the experimental results, but a detailed comparison will be deferred to a later section.

To supplement the numerical solutions, it is helpful to set down several exact deductions from (5) and (7). The single 'stagnation point' for the relative flow outside the sphere (i.e. the point which stays in the same relative position with respect to the sphere) is found by setting the right-hand sides of (5) equal to zero; the only solution for $\alpha = \frac{1}{4}$, $\rho > 1$ is $\theta = \pi$, $\rho = 1{\cdot}11$ approximately. Inside the spherical vortex there are three such points for $\alpha = \frac{1}{4}$, one at $\theta = 0$, $\rho = 0{\cdot}92$ on the central axis, and the other two at $\rho = 1/\sqrt{2} = 0{\cdot}708, \theta = \pm 76\frac{1}{2}°$. These latter are of course the points about which the internal circulation is taking place relative to the expanding sphere. They are at the same radius as the corresponding stagnation points for a spherical vortex of fixed size, but are moved forward slightly in the co-ordinate system used here, through a distance which depends on the angle of spread α.

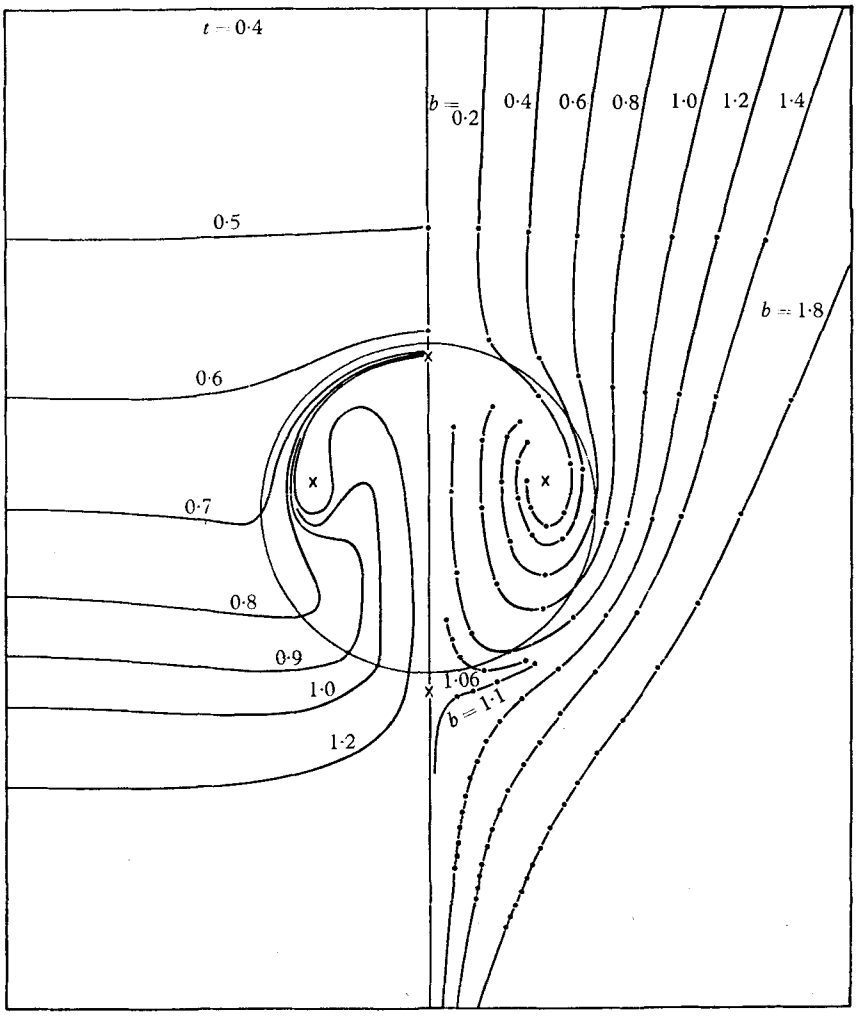

FIGURE 4. The motion of particles into an expanding spherical vortex, plotted using a co-ordinate system in which the spherical boundary is fixed in size. The tangent of the half-angle of spread is $\alpha = \frac{1}{4}$. The right side of the diagram shows the paths of particles which started on a plane at right angles to the direction of motion. The points marked are separated by equal time intervals if the vortex has a constant forward velocity. The left side of the diagram shows the successive shapes into which a plane of fluid is distorted by the passage of the vortex.

5. Distribution of the inflow

Let us now look in more detail at the history of particles which enter the spherical vortex. In the absence of the sphere, but using the expanding co-ordinate system, all particles would converge along straight lines to a 'virtua origin' at $\theta = \pi, \rho = 1/\alpha$ or $\rho = 4$ for the case plotted in figure 4. The transverse position of particles at large distances may conveniently be scaled in terms of the intercepts b cut off by these converging paths on the plane $\theta = \frac{1}{2}\pi$ which passes through the centre of the sphere. Alternatively we can use the initial angle of approach to the virtual origin, β say, given by $\tan\beta = \alpha b$.

The angular distance θ from the front of the spherical vortex to the point of entry of a particle into the sphere is shown as a function of β in figure 5. Note that, for $\alpha = \frac{1}{4}$, particles out to just less than $\tan\beta = \alpha b = 0{\cdot}275$ enter the sphere. The volume of external fluid eventually incorporated is greater than would be judged by drawing the tangent cone to the sphere at a particular instant; the value of α corresponding to the tangent is also shown on figure 5.

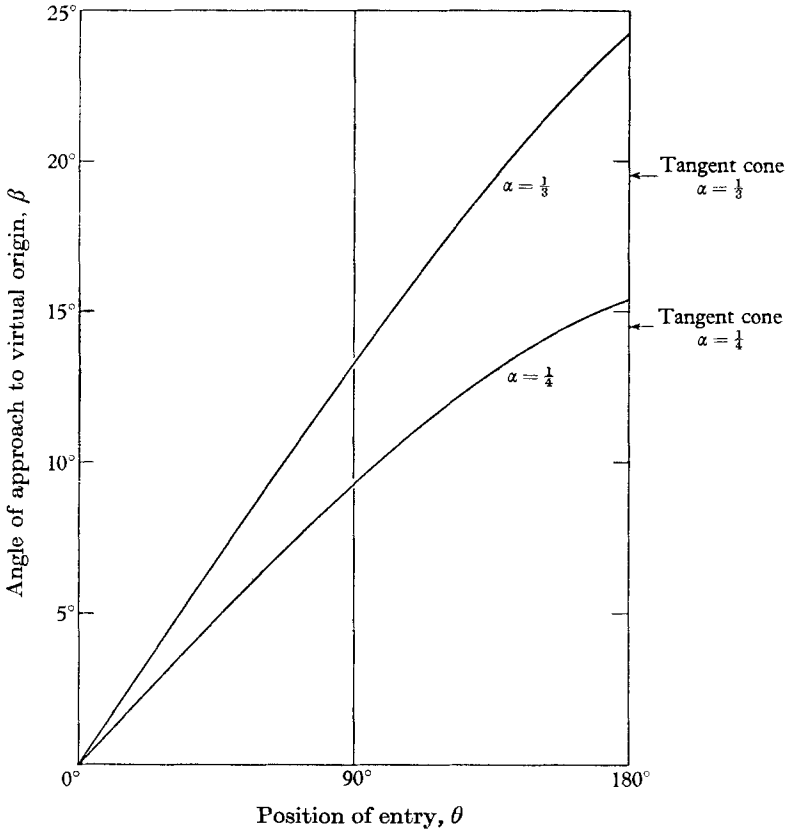

FIGURE 5. The initial angle of approach of particles towards the virtual origin, plotted against their final positions of entry into an expanding vortex (as specified by the angular distances from the front). Results are shown for two half angles of spread, $\alpha = \frac{1}{4}$ and $\alpha = \frac{1}{3}$, and the angles of the tangent cones are also marked.

Another quantity which has been deduced from laboratory measurements is the proportion of external fluid which enters over the front of the thermal (from $\theta = 0$ to $\theta = \pm\frac{1}{2}\pi$). In considering the corresponding calculation for an expanding spherical vortex, we must be careful to specify exactly what is meant. In our model, the instantaneous inward flux of fluid is of course the same everywhere over the sphere, so that we can say immediately that 50 % of the entering fluid comes in at the front. It might perhaps be argued that it is possible to define the proportions in another way which depends on the relative volumes of the conical regions from which fluid is drawn over a long

time, but this is less realistic because of the different times at which particles on different streamlines enter the sphere.

One would expect that the results shown in figure 5 could depend on the angle α, so for comparison the computation of particle paths outside the sphere has been repeated for $\alpha = \frac{1}{3}$. The general form is similar to figure 4 and will not be given in detail, but it has been used to prepare the second curve on figure 5. With $\alpha = \frac{1}{3}$, particles even further off the axis eventually enter the sphere; the rear stagnation point corresponds to $\tan\beta = \alpha b = 0{\cdot}45$ approximately.

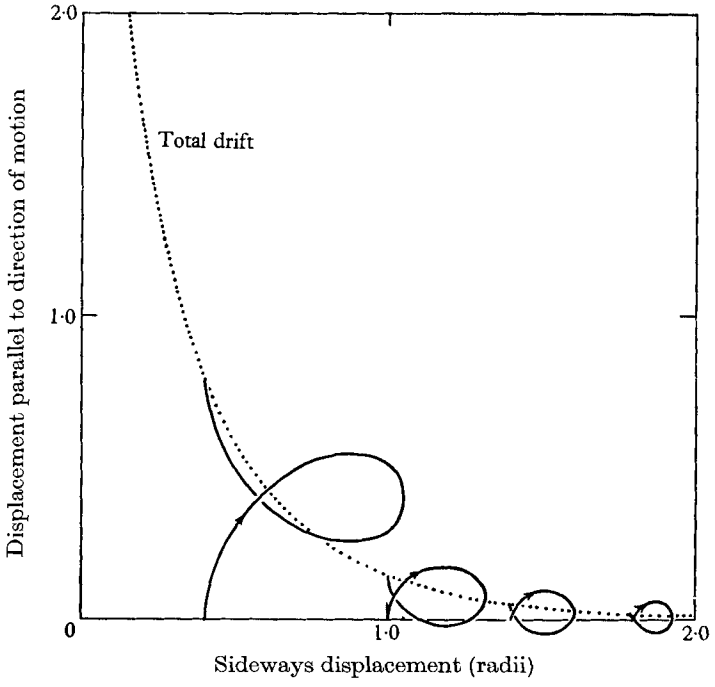

FIGURE 6. Displacements of particles in a frictionless fluid, caused by the passage of a solid sphere. Also shown is the 'total drift function', or locus of the final displacements in the direction of motion of the sphere (which is upwards).

If α is increased still further, the rear stagnation point disappears altogether. It may be deduced from equations (5) that this occurs for $\alpha > 0{\cdot}47$, rather larger than is relevant for the comparison with experiment we are attempting here. The result seems worth recording however; it implies that, given long enough and a certain minimum angle of spread, *all* exterior particles will become incorporated in the expanding spherical vortex.

6. Motions of particles relative to axes at rest

So far the results of the computations on the expanding vortex have all been given relative to co-ordinates fixed in the spherical vortex and expanding with it. We shall now superpose the velocity of the vortex and plot the paths of particles relative to the fluid at rest, and consider how these paths are affected by the expansion.

For a spherical vortex of constant size, or a solid sphere in a frictionless fluid, typical particle paths may be calculated by extending the results of Lighthill (1956). These are shown in figure 6; they are symmetrical looped curves, with

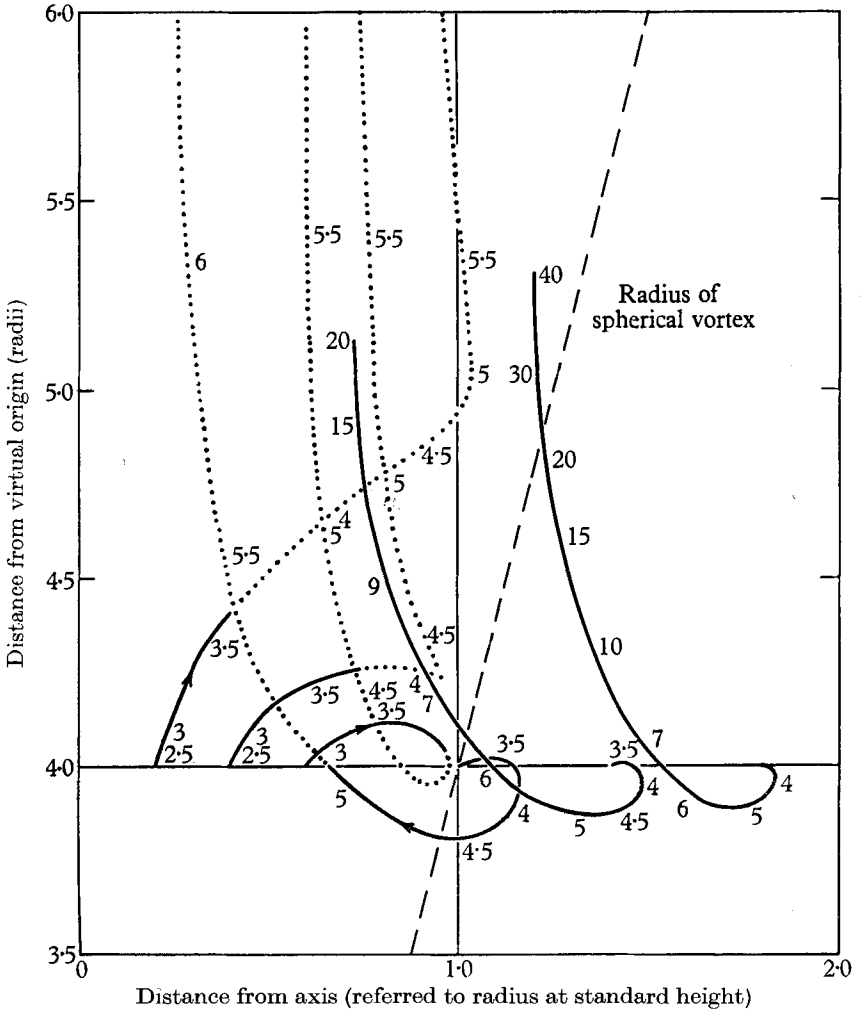

FIGURE 7. The displacement of fluid particles relative to axes at rest, due to the passage of a spherical vortex whose radius is increasing linearly with distance. Distances are measured in units of the radius of the vortex as its centre passes through the plane where the particles are originally distributed. The numbers on the curves refer to the height of the centre when the particle has reached the marked position. Full lines: particles moving outside the vortex; dotted lines: inside.

the particles moving first up and outwards, and then down and in again. There is a finite net displacement in the direction of motion of the sphere, and the locus of final positions, or the 'total drift function', is also plotted.

The behaviour of particles near an expanding sphere is very different, as shown in figure 7. The initial positions have been chosen to lie on a plane at distances from the axis which are various fractions of the radius of the vortex

as its centre passes through this plane. The numbers on the curves represent the position of the sphere (in units of the standard radius from the virtual source) when the particles have reached the points marked. Particles near the axis move up and out before being incorporated into the sphere, and their paths inside the spherical vortex are continued as dotted lines. Further out, some downward motion occurs before a particle enters the spherical vortex from the rear, and particles which never enter the sphere move downwards before being drawn up into the wake of the vortex.

It appears that there is a fundamental difference here from the calculation for a sphere of constant size, in that there is *no* position corresponding to the 'total drift' of a particle. That is, so long as the expanding sphere is moving, particles near the axis will still have a finite upward velocity. This may be demonstrated as follows. Using Lighthill's notation, the 'drift' X is defined by $X = t+x$, where x is the relative displacement in the direction of motion, and the upward velocity is taken as unity. For particles near the axis and behind the vortex, $\theta \approx \pi$ and $x \approx -r$, so that the first of equations (3) may be written

$$\frac{dX}{dt} = \frac{\alpha^3 t^3}{r^3} = \frac{\alpha^3}{(1-X/t)^3}. \tag{8}$$

Thus if X is finite and t becomes large

$$dX/dt = \alpha^3; \tag{9}$$

the upward particle velocity remains a finite fraction of the velocity of the vortex, except for $\alpha = 0$, which corresponds to a sphere of constant size. To the same order of approximation, the particles will at large times be moving parallel to the direction of motion of the vortex.

7. Discussion

We shall now return to a comparison of the calculated particle motions with what has been found in laboratory experiments. To what extent can the mean motions we have derived account for the observed behaviour in a turbulent buoyant thermal?

A comparison of the stream functions and velocity components with respect to axes at rest has already been carried out. We can now compare directly the relative streamlines and the distortion of initially plane surfaces shown in figure 4 with the corresponding results given by Woodward in her figures 4 and 5. The agreement is good, except that again there is the suggestion that the laboratory thermals are more nearly oblate spheroids than spheres.

It is possible to go further and explain the existence of the thin layer of mixing near the front of the thermal, in terms of the mean flow pattern. In figure 4, the front stagnation point lies only a short distance inside the boundary of the moving spherical region, so fluid entering over the front will not penetrate far, but will be swept sideways round the outer layers of the cap. In addition, of course, this fluid will be unstable with respect to the interior of the thermal, and enhanced turbulent mixing may occur near this layer. In cases where the

buoyant fluid is confined to a ring which does not extend out to the cap, there is no instability at the front of the spherical volume moving with the vortex ring, and the flow can remain smooth, as previously observed by Turner (1957). Even in the turbulent case, however, the symmetry of streak pictures like figure 1 shows that the differences between the motion at the front and rear are not large, and that our interpretation depends greatly on the co-ordinate system in which we view the thermal.

The addition of external fluid over a broad region at the rear is also to be expected from figure 4. Here the density stratification produced by the mean motion is either stable or neutral; an overturning is not produced until the added fluid has moved up the centre towards the front of the thermal, so the density differences will not enhance the mixing at the rear. The existence of this general upflow in the middle of the thermal suggests that the buoyant fluid could be confined to only part of the moving region, and that the shape of the fluid moving with the vortex may be more nearly spherical than the outline of dye. Some flattening, however, is also apparent from the streamlines as we have already noted.

The fraction of fluid added over the front of the spherical vortex, which is exactly $\frac{1}{2}$ using our model, is at the bottom end of the range of values $\frac{1}{2}$–$\frac{2}{3}$ suggested by Miss Woodward from her experiments. As she pointed out, however, these figures do depend on the variations of the position of the edge of thermals due to turbulent fluctuations, which may trap fluid closer to the front.

It can now be stated with some confidence that the main features of the motion in and around a buoyant thermal can be explained very well using the expanding vortex model. The flow outside can be described closely by the potential flow around a solid sphere of the same size, and that inside by the distribution in Hill's spherical vortex. Two qualifications to this statement must be made: experimental thermals are flattened slightly, and the mean velocity distributions so far measured do not show the discontinuity of gradient which is implied by the spherical vortex model.

Apart from its special application, the picture which emerges from these calculations may be of more general interest, for it represents a case where an inviscid-flow solution should remain valid in real fluids. One is familiar with the use of potential-flow solutions in aerodynamics, where friction has to be considered only in a boundary layer near the body. In the flow considered here, potential flow should remain a good approximation right up to the boundary of the spherical vortex, because not only is the surface moving, but any boundary layer formed is immediately incorporated into the sphere. Thus as far as the external motion is concerned, viscosity can be neglected, and the only resistance to motion of the spherical vortex arises because of the addition or displacement of external fluid which has to be accelerated from rest.

This work was completed during the author's tenure of the Rossby Memorial Fellowship at Woods Hole Oceanographic Institution.

It is Contribution No. 1405 of Woods Hole Oceanographic Institution, and

was supported in part by NSF Contract No. GP-317. I am grateful to Dr P. M. Saunders for his helpful comments on an earlier draft of this paper, and for the photograph which is reproduced in figure 1.

REFERENCES

DARWIN, C. G. 1953 *Proc. Camb. Phil. Soc.* **49**, 342.
LAMB, H. 1932 *Hydrodynamics.* Cambridge University Press.
LEVINE, J. 1959 *J. Meteor.* **16**, 653.
LIGHTHILL, M. J. 1956 *J. Fluid Mech.* **1**, 31.
MORTON, W. B. 1913 *Proc. Roy. Soc.* A, **89**, 106.
SAUNDERS, P. M. 1962 *Tellus*, **14**, 177.
SCORER, R. S. 1957 *J. Fluid Mech.* **2**, 583.
TURNER, J. S. 1957 *Proc. Roy. Soc.* A, **239**, 61.
WOODWARD, B. 1959 *Quart. J. Roy. Met. Soc.* **85**, 144.

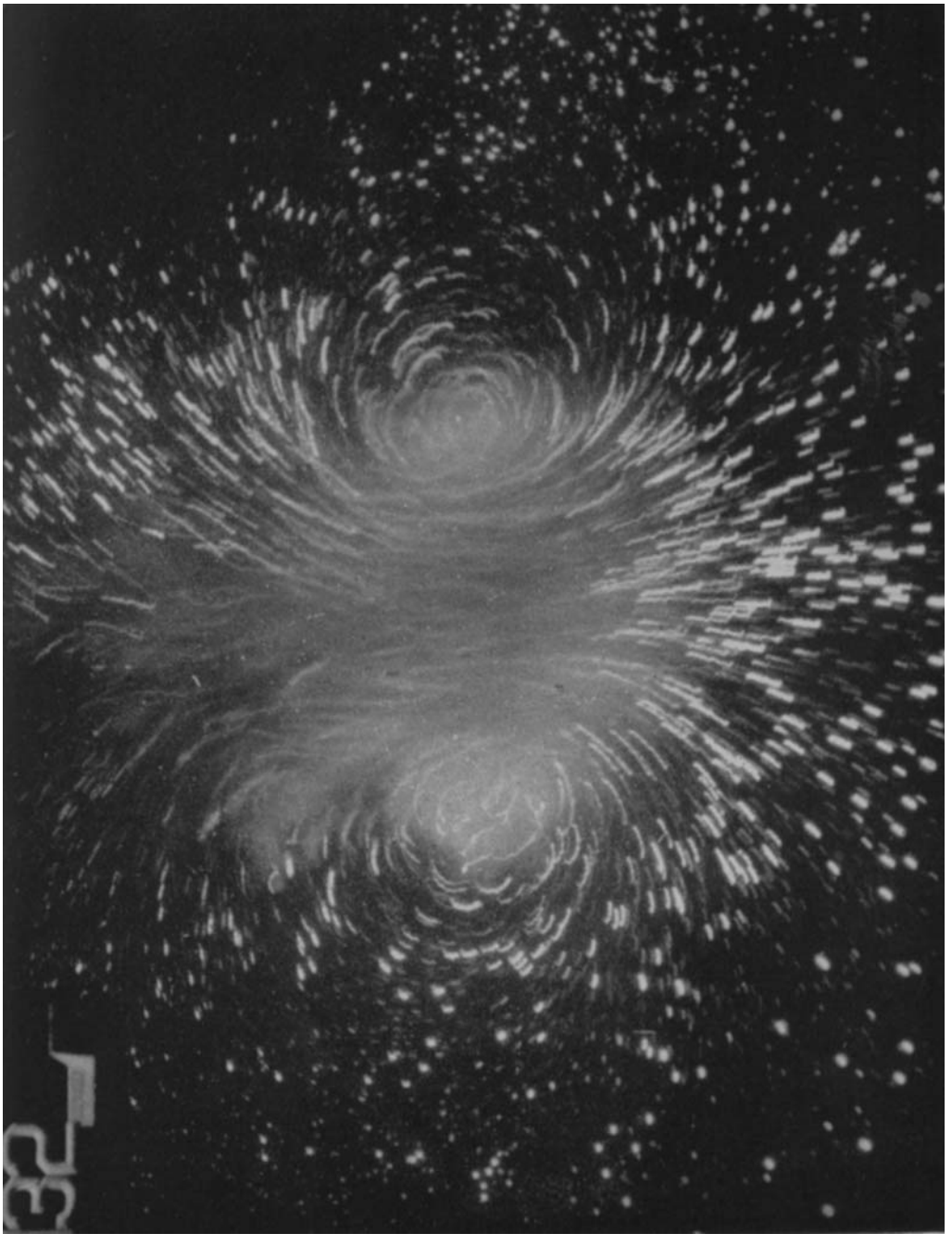

FIGURE 1. Streak picture of the flow in and around an isolated thermal. The exposure time (about $\frac{1}{2}$ sec) is short enough for this to give a good representation of the streamlines relative to axes at rest. The direction of motion in this experiment is downwards; note, however, that all the other diagrams are drawn for upward motion of the spherical vortex.